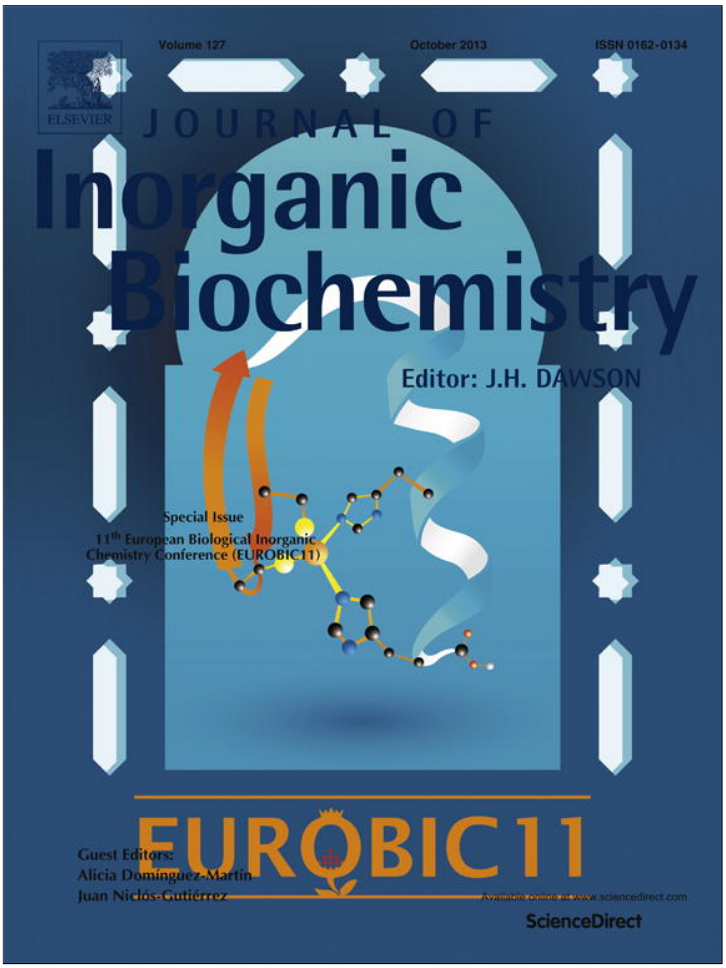

Journal of Inorganic Biochemistry 127 (2013) 232–237

Contents lists available at ScienceDirect

Journal of Inorganic Biochemistry

journal homepage: www.elsevier.com/locate/jinorgbio

Copper-substituted forms of the wild type and C42A variant of rubredoxin

Anders Thapper [a], Alberto C. Rizzi [b], Carlos D. Brondino [b,*], Anthony G. Wedd [c,1], Ricardo J. Pais [d,2], Biplab K. Maiti [d], Isabel Moura [d], Sofia R. Pauleta [d,**], José J.G. Moura [d,3]

[a] Department of Photochemistry and Molecular Science, Uppsala University, P.O. Box 523, S-751 20 Uppsala, Sweden
[b] Departamento de Física, Facultad de Bioquímica y Ciencias Biológicas, Universidad Nacional del Litoral, S3000ZAA Santa Fe, Argentina
[c] School of Chemistry and Bio21 Molecular Science and Biotechnology Institute, University of Melbourne, Parkville, Victoria 3010, Australia
[d] REQUIMTE-CQFB, Departamento de Química, Faculdade de Ciências e Tecnologia, Universidade Nova de Lisboa, 2829-516 Caparica, Portugal

ARTICLE INFO

Article history:
Received 24 November 2012
Received in revised form 3 May 2013
Accepted 5 June 2013
Available online 13 June 2013

Keywords:
Rubredoxin
Mutant coordination site
Copper-substituted iron–sulfur center
UV–visible
EPR

ABSTRACT

In order to gain insights into the interplay between Cu(I) and Cu(II) in sulfur-rich protein environments, the first preparation and characterization of copper-substituted forms of the wild-type rubredoxin (Rd) from *Desulfovibrio vulgaris* Hildenborough are reported, as well as those of its variant C42A-Rd. The initial products appear to be tetrahedral $Cu^{I}(S–Cys)_n$ species for the wild type (n = 4) and the variant C42A (n = 3, with an additional unidentified ligand). These species are unstable to aerial oxidation to products, whose properties are consistent with square planar $Cu^{II}(S–Cys)_n$ species. These Cu(II) intermediates are susceptible to auto-reduction by ligand S–Cys to produce stable Cu(I) final products. The original Cu(I) center in the wild-type system can be regenerated by reduction, suggesting that the active site can accommodate $Cu^{I}(S–Cys)_2$ and Cys–S–S–Cys fragments in the final product. The absence of one S–Cys ligand prevents similar regeneration in the C42A–Rd system. These results emphasize the redox instability of $Cu^{II}–(S–Cys)_n$ centers.

1. Introduction

Copper is an essential element present in the structure of electron transfer proteins, such as plastocyanin and azurin, and in redox enzymes, such as cytochrome *c* oxidase, nitrite reductase, and superoxide dismutase [1,2]. These proteins accomplish their functions using the Cu(II)/Cu(I) couple with redox potentials in the range 0–1000 mV (*vs* SHE, Standard Hydrogen Electrode). Most of the Cu(II)/Cu(I) redox potentials in proteins fall in the range 200–300 mV, rather different to that of the aqua-Cu(II)/Cu(I) couple (159 mV), which, however, determines that under aerobic conditions the copper ion in these proteins is present mostly as Cu(II). The higher redox potential found in proteins is determined by factors, such as, the active site structure, hydrogen bonding pattern around the active site, and the electrostatic environment [3]. Although copper is an essential element, it must be tightly regulated, as the free ions can catalyze oxidative damage via radical formation [4] or can induce cell damage by ligation to the coordinating sulfur atoms in Fe–S clusters [5]. Such problems are avoided by the presence of high affinity copper proteins, such as copper trafficking proteins and copper metallothioneins, that control the copper levels [6–9]. In these proteins, copper is normally present as Cu(I) [10,11], which indicates that these copper centers have high redox potentials, likely related to the sulfur-rich environment of the copper ions. Many trafficking proteins show a conserved *CXXC* motif that incorporates one copper atom per molecule, in which S-cysteines are the copper ligands [12–14]. S-cysteines are also the ligands in metallothioneins, which can incorporate up to 7 copper atoms per molecule [15]. Fe–S clusters can also bind a copper atom yielding a stable product, demonstrating the chemical feasibility of CuFeS clusters, which suggests that this kind of clusters could exist naturally in biological systems [16]. Although several crystallographic studies demonstrated the versatility of Cu(I) coordinated by sulfur-rich environments [17–20], questions, such as the chemical changes suffered by the proteins leading to the stabilization of Cu(I) under aerobic conditions are, in our opinion, virtually unstudied. Hence, the investigation of coordination chemistry of copper(I) using appropriate systems featuring S–Cu interactions is relevant to a detailed molecular understanding of copper sites in proteins.

Sulfur-rich metal coordination sites are found in iron–sulfur centers (mono-, bi-, tri-, and tetranuclear iron sites and their structural variations). Rubredoxins (Rd) are the simplest iron–sulfur proteins (with a molecular mass of 5.6 kDa) and contain a single iron atom tetrahedrally coordinated by the sulfur atoms of four cysteine residues arranged in a – $C_6X_2C_9–X_n–C_{39}X_2C_{42}$ – motif [21]. The *CXXC* motif is also found in most Atx1 homologues, which possess a ferredoxin-like fold [8]. The iron atom in rubredoxin can be substituted by other metal ions by acid precipitation of the protein and reconstitution

* Corresponding author. Tel.: +54 342 4575213; fax: +54 342 575221.
** Corresponding author. Tel.: +351 212948385; fax: +351 212948550.
E-mail addresses: brondino@fbcb.unl.edu.ar (C.D. Brondino), srp@fct.unl.pt (S.R. Pauleta), jose.moura@fct.unl.pt (J.J.G. Moura).
[1] Visiting Gulbenkian Foundation Professor at REQUIMTE.
[2] Present address: CQB, Departamento de Química e Bioquímica, Faculdade de Ciências, Universidade de Lisboa, 1749-016 Lisboa, Portugal.
[3] Tel.: +351 212948382; fax: +351 212948550.

0162-0134/$ – see front matter © 2013 Elsevier Inc. All rights reserved.
http://dx.doi.org/10.1016/j.jinorgbio.2013.06.003

in basic media under reducing conditions. Furthermore, variants of rubredoxins where one of the four cysteines is replaced by a potential ligand (serine) or a non-ligand (alanine) have been prepared previously by site-directed mutagenesis and characterized spectroscopically [22–25]. Overall, metal-substituted rubredoxins containing ^{57}Fe(II), Co(II), Ni(II), Zn(II), Cd(II), Hg(II), Ga(III) and In(III) have been prepared and characterized [21,26,27]. However, the preparation of copper-substituted rubredoxins has remained elusive.

The above discussion suggests that copper-substituted rubredoxins may constitute a useful model system to investigate copper (II/I) stability in protein sulfur-rich coordination environments. In the present work, we report the preparation and characterization of the copper-containing forms of the wild-type *Desulfovibrio (D.) vulgaris* Hildenborough rubredoxin and its C42A variant. Our results show that copper can be incorporated as copper(I) in these systems. The initial forms are unstable in air and pass through copper(II) intermediates prior to generation of stable copper(I) species with properties different from the initial ones. The latter can be converted back to the initial form for the wild-type protein but not for the C42A variant.

2. Materials and methods

2.1. Reagents

$CuCl_2 \cdot 2H_2O$, $FeCl_2 \cdot 4H_2O$, dithiothreitol (DTT), β-mercaptoethanol and trichloroacetic acid (TCA) were purchased from Merck. Luria–Bertani (LB) medium, neomycin, ampicillin and isopropyl-β-D-thiogalactopyranoside (IPTG), were from Sigma. All buffers and reagents were of the highest commercially available grade. All solutions were prepared in Milli-Q water.

2.2. Protein production

The expression vector for C42A rubredoxin was obtained by site directed mutagenesis, using the "QuickChange Site-Directed Mutagenesis Kit" (Stratagene). The expression vector pT7-7/RdDv was used as template and the primers were designed according to the manufacturer's instructions. In order to verify the incorporation of the mutation, the mutated expression vector was sequenced. The heterologous production of the wild-type and C42A *D. vulgaris* Hildenborough rubredoxin followed the procedure described for *D. vulgaris* desulforedoxin [28]. In short, competent *Escherichia coli* BL21(DE3) (Novagen) were transformed with the expression vectors pT7-7/RdDv or pT7-7/RdDvC42A. The cells were grown in an orbital shaker at 37 °C in LB medium, supplemented with 0.1 mg/mL ampicillin and 0.1 M $FeCl_2 \cdot 4H_2O$, until an absorbance at 600 nm of 0.8. Protein production was induced with 1 mM IPTG, at 25 °C for 18 h. The cells were harvested by centrifugation at 2500 ×*g* for 15 min, and resuspended in 10 mM Tris–HCl, pH 7.6.

2.3. Isolation of the wild-type and C42A rubredoxin from *D. vulgaris Hildenborough*

The soluble cell extract was obtained by 4 passages in a French Pressure Cell at 15000 psi and centrifuged at 20000 ×*g* for 90 min. The supernatant was loaded onto a DEAE-52 (Sigma) anion exchange column equilibrated with 10 mM Tris–HCl, pH 7.6. The proteins were eluted with a gradient between 0 mM and 500 mM NaCl in 10 mM Tris–HCl, pH 7.6. The fractions containing the wild-type or the mutant rubredoxin were combined and concentrated. The second and final chromatographic step involved a gel filtration chromatography, using a Superdex 75 (GE HealthCare) equilibrated with 50 mM Tris–HCl, pH 7.6, 150 mM NaCl. The fractions containing pure rubredoxin were combined and concentrated. Throughout the purification the purity of the wild-type and mutant rubredoxin fractions was assessed by 15% polyacrylamide Tris-Tricine SDS-PAGE and UV–visible spectroscopy.

2.4. Metal substitution

Iron containing C42A rubredoxin (Fe–C42A–Rd) was prepared following the procedure of Moura et al. [29]. Copper-substituted wild-type (Cu–Rd) and C42A (Cu–C42A–Rd) rubredoxins were prepared from Fe–Rd and Fe–C42A–Rd, respectively, using an adapted procedure of that method, in which the protein was precipitated at 50 °C with 5% TCA in the presence of 0.5 M β-mercaptoethanol. The protein precipitate was centrifuged at 6000 rpm and resuspended in 0.5 M Tris base and 60 mM β-mercaptoethanol. In order to minimize iron contamination, this precipitation was repeated twice at room temperature. The final protein precipitate was resuspended to a concentration of about 15 mg/mL in 0.5 M Tris base containing 60 mM DTT, and incubated for 30 min under argon at room temperature. Finally, one equivalent of $CuCl_2 \cdot 2H_2O$ was added, and incubated for 10 min under argon followed by 1 h in air. The copper-substituted rubredoxins were passed through a NAP-5 column (GE HealthCare) equilibrated with 10 mM Tris–HCl, pH 7.6 to separate the protein from any unbound metal. The samples were subjected to buffer exchange via centrifugation over a 3 kDa cut off centricon (Vivaspin, Sartorius) to remove free metal ions. The same procedure performed without the presence of DTT in the buffer showed the same level of copper ion incorporation into the proteins.

2.5. Metal and protein determination

The total amount of copper, iron and zinc present in solution was estimated using an inductively coupled plasma (ICP) atomic emission spectrometer. Protein content was performed by the bicinchoninic acid colorimetric assay (Sigma) or a modified version of the Folin-Biuret method, using *Desulfovibrio gigas* rubredoxin as standard [30].

2.6. Spectroscopic measurements

UV–visible absorption data were collected on a Shimadzu UV-2101PC split beam spectrophotometer using 1 cm optical path quarts cells. The extinction coefficients of Cu–Rd and Cu–C42A–Rd were determined based on the copper quantification. EPR-spectra were recorded on a Bruker EMX spectrometer equipped with an Oxford Instruments helium continuous-flow cryostat. EPR spectra were collected at temperatures between 4 and 80 K at 9.65 GHz under non-saturating conditions. Spin quantification of Cu–Rd and Cu–C42A–Rd signals was performed using 3 mM cupric EDTA as a standard. Computer simulations of the spectra were performed using the program SIMPOW6 [31].

3. Results and discussion

3.1. Fe-containing wild type and C42A variant proteins

The wild-type *D. vulgaris* Hildenborough rubredoxin and the single point variant C42A–Rd (which lacks the iron ligand C42) were heterologously produced in *E. coli* BL21(DE3). The wild-type form (Fe–Rd) was obtained as a mixture of the ruby Fe(III) form (93%) and the colorless Zn(II) form (7%). On the other hand, C42A–Rd purified essentially as the colorless Zn(II) form (97%) with a small fraction of the Fe(III) form (3%). These two proteins migrated in reducing and non-reducing SDS-PAGE as 6 kDa proteins (data not shown), and its metal/protein ratio gives no evidence for the presence of apo-protein. This result contrasts with that for the C42A mutant from *Clostridium* (*C.*) *pasteurianum*, which was purified with a 2Fe–2S cluster [23,32], that could be converted to a stable Fe(III) form (Fe–C42A–Rd) by metal substitution [23,32].

The UV–visible spectrum of Fe–Rd (Fig. 1A) is similar to that reported for the protein purified from a soluble extract of the same bacterium [33]. The EPR spectrum shows a resonance at g ~ 9.5 plus a narrow signal at g ~ 4.3 superimposed on a broad signal in the

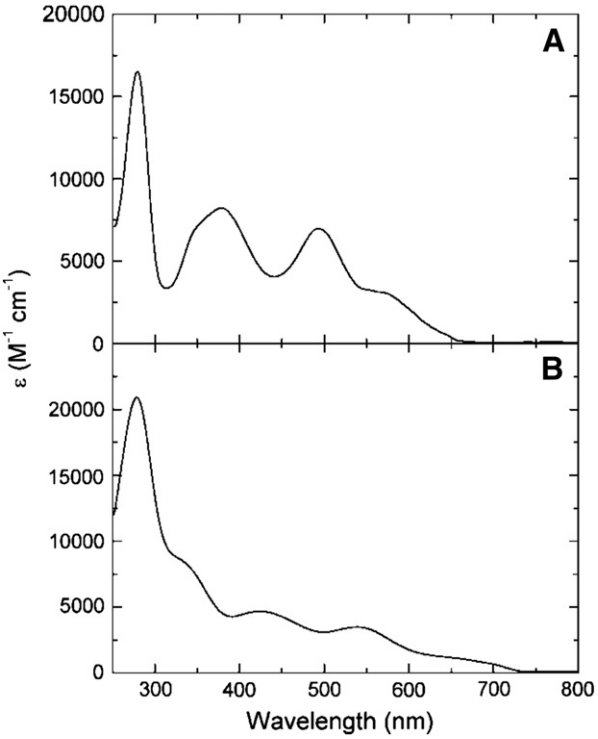

Fig. 1. UV–visible spectra of Fe–Rd (A) and reconstituted Fe–C42A–Rd (B) in 10 mM Tris–HCl, pH 7.6.

range g ~ 4.6–4.0 (Fig. 2). This spectrum, similar to those observed in other bacterial rubredoxins, is typical of a high-spin Fe(III) center possessing a large zero-field splitting and high rhombic distortion ($E/D \approx 1/3$, $D > 0$) [34,35].

The UV–visible spectrum of the reconstituted Fe–C42A–Rd (Fig. 1B) presents a shoulder at ~340 nm and two broad absorption bands at 425 nm (4600 M^{-1} cm^{-1}) and 539 nm (3500 M^{-1} cm^{-1}). Compared to that of Fe–Rd, this spectrum exhibits broader and less intense absorption maxima that are mostly shifted to higher energies. Such properties are consistent with lower site symmetry and the presence of fewer than four Cys ligands to Fe(III) [23]. The EPR spectrum exhibits absorptions at

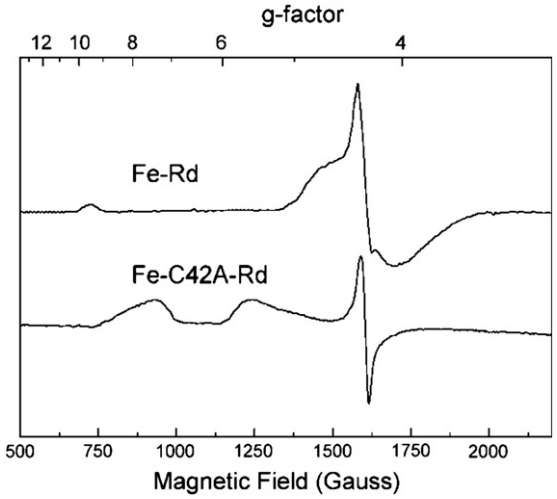

Fig. 2. EPR spectra of Fe–Rd (upper) and Fe–C42A–Rd (lower) in 10 mM Tris–HCl, pH 7.6. Experimental conditions: temperature, 4 K; microwave frequency, 9.65 GHz; modulation amplitude, 5.0 G.

g ~ 7.8, 5.5 and 4.3 (Fig. 2), similar to those reported for center I of the C42A mutant rubredoxin from *C. pasteurianum* (g ~ 7.3, 5.7, and 4.3) [23] and also to the g-values of center I in *D. gigas* desulforedoxin (resonances at g ~ 7.3, 5.7 and broad feature at g ~ 4) [36]. Following Cross et al., these spectra correspond to Fe(III) sites with $E/D < 0.1$ where the iron center is assigned to a tetrahedral $Fe^{III}(S\text{–}Cys)_3(OH)$ center [23].

3.2. Copper-substituted wild type and C42A variant proteins

Cu–Rd and Cu–C42A–Rd forms were prepared using a modification of the methodology developed to substitute the Rd Fe-center for other metals (Ni, Co, Cd) [29]. Copper was added as $CuCl_2$ to the *apo*-protein in the presence of DTT as reducing agent (in a DTT-protein ratio of 10:1). The resulting solution was colorless, consistent with reduction to Cu(I). The product proteins were desalted using size-exclusion chromatography (see the Materials and methods section). During the elution, Cu–Rd changed color to reddish brown, while Cu–C42A–Rd emerged as a light blue band. Elemental analysis indicated a Cu-protein ratio of 0.9 ± 0.1 for both Cu–Rd and Cu–C42A–Rd.

Upon standing, the colors of both proteins intensified, reaching a maximum after approximately 1 h. This behavior suggested progressive oxidation to Cu(II). However, these forms were also not stable and lost color after several hours of exposure to air. A similar result was obtained when $CuCl_2$ was added to wild-type apo-Rd in the absence of a reducing agent, indicating that copper can enter as Cu(I) or Cu(II). The only difference between both processes is that the maximum of the color is reached earlier (~20 min of incubation), which is reasonable since copper is incorporated as Cu(II) directly.

After removing free copper (see Material and methods: Metal substitution), elemental analysis confirmed that ~0.6 and ~0.7 equivalents of the copper remained bound to the final products for Cu–Rd and Cu–C42A–Rd, respectively.

SDS-PAGE performed under reducing conditions showed a single band of apparent molecular mass of ~6 kDa for both proteins, in line with the results obtained for Fe–Rd and Fe–C42A–Rd. The same result was obtained for Cu–Rd (6 kDa) under non-reducing conditions, while for Cu–C42A–Rd, in addition to the band of 6 kDa, were observed bands of higher molecular mass (with prevalence for one with ~12 kDa) (Supplementary Material, Fig. S2). This result can be explained by the formation of intermolecular disulfide bridges in the mutant Cu–C42A–Rd, which do not occur in the wild type Cu–Rd. Therefore, this suggests that the wild-type does not have the propensity to aggregate due to the formation of an intermolecular disulfide bridge (see the discussion below).

The UV–visible spectra of the intermediate products when copper is incorporated under reducing conditions were obtained after desalting and exposure to air. Copper is almost completely as Cu(II) in Cu–Rd and Cu–C42A–Rd after ~1 and 1.5 h, respectively, of aerial oxidation, as determined from EPR spin quantification (0.9 spin/molecule for both proteins). The spectrum of Cu–Rd (Fig. 3A) exhibits three absorption bands at 355 nm (1900 M^{-1} cm^{-1}), 432 nm (1500 M^{-1} cm^{-1}), and 739 nm (650 M^{-1} cm^{-1}), and a shoulder around 490 nm. In the case of Cu–C42A–Rd, the spectrum presents an absorption band at 627 nm (430 M^{-1} cm^{-1}) and a shoulder at 422 nm (Fig. 3B). These spectra are different to those observed for a solution of Cu(II)/DTT in the absence of protein [37], indicating that the observed bands are not associated with exogenous thiols which could compete with the cys ligands for Cu(II) or Cu(I).

The lowest energy bands are more intense than normally encountered for d–d transitions in Cu(II) (~50 M^{-1} cm^{-1}) but significantly less intense than the S(Cys) to Cu(II) LMCT bands with ε-values *ca.* 3000–5000 M^{-1} cm^{-1} that are observed for blue copper proteins [3]. Copper(II) model complexes with predominantly thiol coordination are very scarce in the literature, presumably because the thiol ligands are prone to be reduced by the copper(II) ion. Macrocyclic thioether ligands have been used to make a series of Cu(II) and

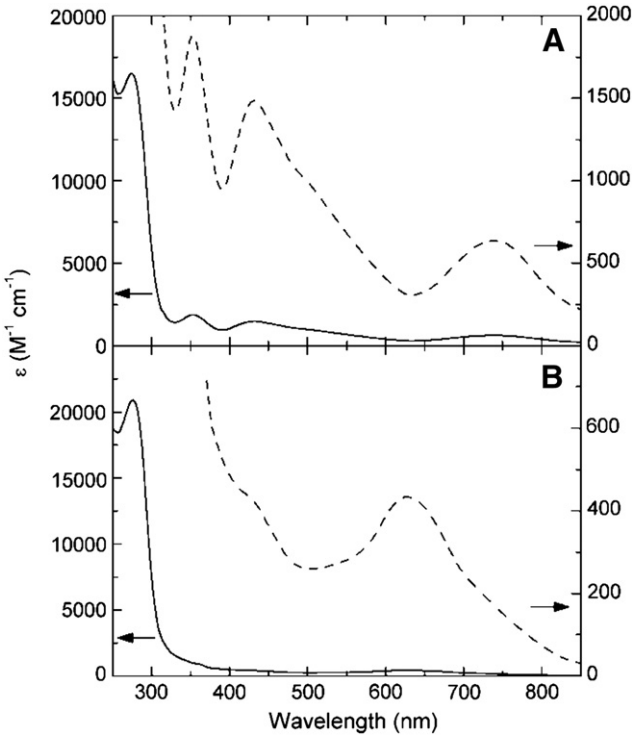

Fig. 3. UV–visible spectra of Cu–Rd (A) and Cu–C42A–Rd (B) in 10 mM Tris–HCl, pH 7.6, after desalting and 60 min exposure to air. Left and right scales correspond to the solid and dash lines, respectively.

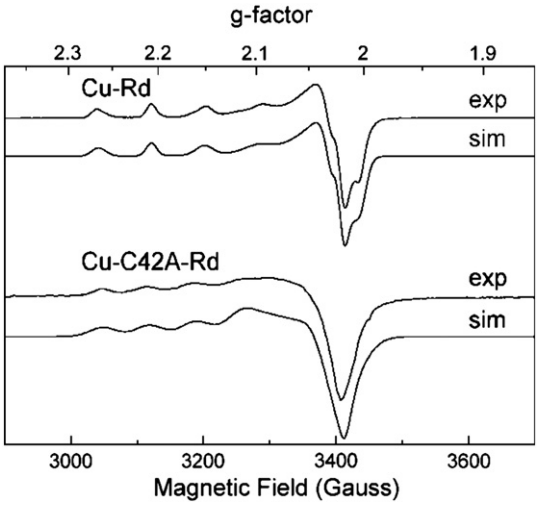

Fig. 4. EPR spectra of Cu–Rd (upper) and Cu–C42A–Rd (lower) in 10 mM Tris–HCl, pH 7.6. Experimental conditions: temperature, 10 K; microwave frequency, 9.65 GHz; modulation amplitude, 5.0 G; exp – experimental; sim – simulation.

Cu(I) complexes where the Cu ion is coordinated by 3–5 sulfur atoms [38]. In the Cu(II) state these complexes adopt a more square-planar or octahedral geometry (with additional solvent molecules coordinating the copper atom), while in the Cu(I) state the geometry is more tetrahedral. The electronic spectra of these complexes had a band around 565–675 nm with ε-values *ca.* 800–2000 M^{-1} cm^{-1} that was suggested to be a S to Cu(II) LMCT band, similar to what is observed for blue copper proteins. In contrast, in a Cu(II) complex with a N3S3 cryptand ligand, a band at 622 nm with ε of 550 M^{-1} cm^{-1} was assigned to three overlapping d–d transitions [39]. For the bands of Cu–Rd and Cu–C42A–Rd, a S(Cys) to Cu(II) LMCT band seems most likely but d–d transitions cannot be completely ruled out. In the former case, the low intensity could come from a less favorable geometry for electronic overlap comparably to blue copper proteins.

The EPR spectra of Cu–Rd and Cu–C42A–Rd are presented in Fig. 4. Both indicate nearly axial symmetry, with well-resolved hyperfine structure in the $g_{||}$ region arising from interactions with the copper nucleus (I = 3/2). Spectral simulations for Cu–Rd were performed assuming roughly axial g-tensors, rhombic anisotropic hyperfine coupling constants and fractional strains in both g- and A-tensors (EPR parameters are given in Table 1). Simulation of the Cu–C42A–Rd spectrum assumed axial and rhombic g- and A-tensors, respectively, without strain. A comparison of the EPR results to those of synthetic Cu(II) complexes and Cu(II)-proteins using the Peisach and Blumberg diagrams [40] suggests a sulfur-rich environment for both Cu–Rd and Cu–C42A–Rd in square planar environments, consistent with the UV–visible spectra. It is likely that the Cu(II) ions are coordinated to all available sulfur ligands, i.e. 4 Cys for Cu–Rd and 3 Cys for Cu–C42A–Rd. Although the $g_{||}$-difference between Cu–Rd and Cu–C42A–Rd is only of the order of 0.01, the larger $g_{||}$-value for Cu–C42A–Rd is suggestive of a less rich sulfur environment. A $Cu(S–Cys)_4$ environment has been observed in the copper-containing Atox1 protein, in which copper is found as Cu(I) [8]. The latter also suggests that a $Cu^{II}(S–Cys)_4$ environment is not stable, as discussed below.

3.3. Reactivity and stability of the copper centers in Cu–Rd and Cu–C42A–Rd

The Cu(II) forms of Cu–Rd and Cu–C42A–Rd were generated by aerial oxidation of the initial Cu(I) species generated under reducing conditions. These forms are also unstable and convert completely to colorless and EPR-silent species after exposure to air for 6 or more hours (EPR spectra as a function of the time are given as Supplementary Material, Fig. S1). This process is slightly slower for Cu–Rd than for Cu–C42A–Rd. The fact that the Cu(II) species are not stable indicates that they have a Cu(II)/Cu(I) redox potential higher than that of the solution under aerobic conditions, i.e. >200 mV, and also suggests that the structure of the Cu(I) species obtained immediately after copper incorporation is different from the Cu(I) species obtained upon longer standing. Since the sequential conversion of unstable Cu(I)–Rd → unstable Cu(II)–Rd → stable Cu(I)–Rd was performed in air, the redox chemistry involved in the second step must necessarily arise from an internal redox process.

In order to obtain further information, DTT was added under anaerobic conditions to the stable form of Cu(I)–Rd to return it to the initial potential at which the metal was incorporated. After air exposure, the reddish brown Cu(II)–Rd was again formed, consistent with the recovery of the initial unstable form of Cu(I)–Rd. In contrast, the same procedure applied to stable Cu(I)–C42A–Rd did not generate the light blue color characteristic of unstable Cu(II)–C42A–Rd. This suggests that the sulfur atom from cysteine 42 is essential for cycling the redox process.

Scheme 1 rationalizes the observations for the wild-type protein. The tetrahedral site $Cu^{I}(S–Cys)_4$ is generated under reducing conditions but is oxidized to a square planar or distorted square planar site $Cu^{II}(S–Cys)_4$ in the presence of O_2. This is unstable due to internal

Table 1
Parameters used in the simulation of the EPR spectra of Cu–Rd and Cu–C42A–Rd.

	Cu–Rd		Cu–C42A–Rd
g_z	2.181 (15)	$\Delta g_z = -0.039$	2.190 (40)
g_y	2.034 (13)	$\Delta g_y = -0.025$	2.051 (56)
g_x	2.026 (20)	$\Delta g_x = 0.251$	2.042 (21)
A_z	117	$\Delta A_z = 0.432$	104
A_y	5	$\Delta A_y = -0.124$	52
A_x	31	$\Delta A_x = -0.364$	7

A-values (for ^{63}Cu) and line widths are given in Gauss. Δg and ΔA represent the g and A strains, respectively. Line widths are given in parentheses. Simulated with both ^{63}Cu (69.2%) and ^{65}Cu (30.8%). A-values for ^{65}Cu are 1.071 times larger than for ^{63}Cu.

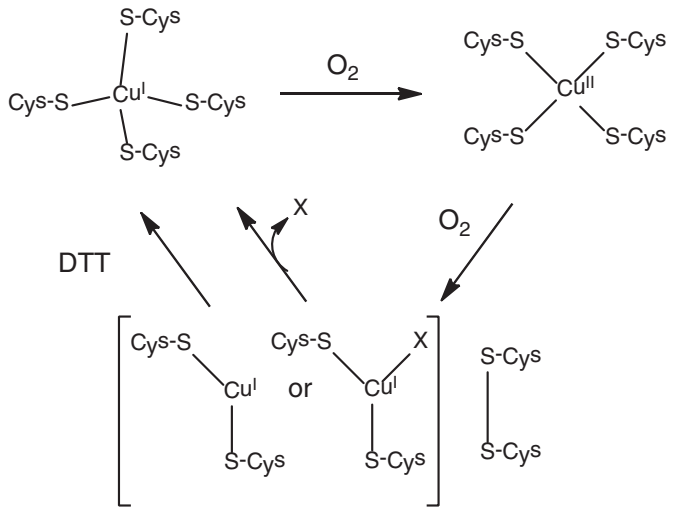

Scheme 1. Proposed changes in Cu-coordination environment during the reversible internal redox process of Cu-Rd.

redox reactions, leading to two-coordinate $Cu^{I}(S–Cys)_2$ or three-coordinate $Cu^{I}(S–Cys)_2X$ centers (X = an unidentified endogenous ligand). This assumes generation of an internal disulfide bond, consistent with the ability of reductant DTT to regenerate the original $Cu^{I}(S–Cys)_4$ site. It should be noted, however, that the Cu content of the Cu(II) forms and final Cu(I) protein products was not stoichiometric. Consequently, at least one step in these processes features a competing side-reaction leading to a state that has lost Cu. The lower number of available Cys sidechains for the C42A system means that greater mechanistic uncertainties hold for this system and no reaction mechanism can be suggested with the present data.

The redox process of Cu–Rd resembles the copper-catalyzed oxidation of the metal-coordinating cysteine sulfur observed in folding studies of azurin and plastocyanin [41,42]. The redox reaction observed in these cupredoxins was described by a reversible equilibrium between native and unfolded molecules followed by a step leading to irreversibly denatured molecules. The redox equilibrium Cu(II)/Cu(I) has also been observed and studied in copper macrocycle complexes [43]. Although the exact nature of the mechanism conducting these internal redox processes remains unclear, our study shows that complex reactions involving reversible and irreversible redox reactions in copper proteins are associated undoubtedly with changes in copper coordination environment.

4. Conclusions

The first preparation and characterization of copper-substituted forms of wild-type rubredoxin and of its variant C42A–Rd are reported. The initial products are Cu(I) forms of the proteins, proposed to be tetrahedral $Cu^{I}(S–Cys)_n$ species (n = 4 for Cu–Rd and n = 3 for Cu–C42A–Rd). These initial Cu(I) forms are unstable to aerial oxidation of the copper site. The oxidized products can be assigned as square planar $Cu^{II}(S–Cys)_n$ species. The Cu(II) forms are in turn susceptible to autoreduction by ligand S–Cys to produce stable Cu(I) final products. The original Cu(I) center in the wild-type system can be regenerated by reduction, suggesting that the active site can accommodate $Cu^{I}(S–Cys)_2$ and Cys–S–S–Cys fragments in the final product. The loss of one S–Cys ligand in C42A–Rd prevents a similar regeneration for its final Cu(I) form.

The overall situation appears to be similar to that seen in copper trafficking proteins, where Cu(I) is stabilized in two- or three-coordinate geometries featuring Cys ligands, imposing a high reduction potential on the metal site which indicates redox instability of the oxidized $Cu^{II}(S–Cys)_n$ site.

Acknowledgments

This work has been supported by Fundação para a Ciência e a Tecnologia (Portugal) through grant No. PEst-C/EQB/LA0006/2011 and, FONCyT, CONICET, and CAI + D-UNL in Argentina. C.D.B is a member of CONICET-Argentina and S.R.P. is a member of REQUIMTE, Associated Laboratory in Portugal, funded by Fundação para a Ciência e a Tecnologia. SRP thanks Fundação para a Ciência e Tecnologia for financial support (PTDC/BIA-PRO/098882/2008).

Appendix A. Supplementary data

Supplementary data to this article can be found online at http://dx.doi.org/10.1016/j.jinorgbio.2013.06.003.

References

[1] E.I. Solomon, U.M. Sundaram, T.E. Machonkin, Chem. Rev. 96 (1996) 2563–2606.
[2] C. Dennison, Coord. Chem. Rev. 249 (2005) 3025–3054.
[3] E.I. Solomon, R.K. Szilagyi, S. DeBeer George, L. Basumallick, Chem. Rev. 104 (2004) 419–458.
[4] B. Halliwell, J.M. Gutteridge, Biochem. J. 219 (1984) 1–14.
[5] L. Macomber, J.A. Imlay, Proc. Natl. Acad. Sci. U. S. A. 106 (2009) 8344–8349.
[6] S.J. Lin, R.A. Pufahl, A. Dancis, T.V. O'Halloran, V.C. Culotta, J. Biol. Chem. 272 (1997) 9215–9220.
[7] L.A. Finney, T.V. O'Halloran, Science 300 (2003) 931–936.
[8] A.K. Boal, A.C. Rosenzweig, Chem. Rev. 109 (2009) 4760–4779.
[9] N.J. Robinson, Nat. Chem. Biol. 4 (2008) 582–583.
[10] N.J. Robinson, D.R. Winge, Annu. Rev. Biochem. 79 (2010) 537–562.
[11] P. Chen, A. Munoz, D. Nettesheim, C.F. Shaw III, D.H. Petering, Biochem. J. 317 (Pt 2) (1996) 395–402.
[12] S.J. Lin, V.C. Culotta, Proc. Natl. Acad. Sci. U. S. A. 92 (1995) 3784–3788.
[13] L.S. Field, E. Luk, V.C. Culotta, J. Bioenerg. Biomembr. 34 (2002) 373–379.
[14] F. Arnesano, L. Banci, I. Bertini, D.L. Huffman, T.V. O'Halloran, Biochemistry 40 (2001) 1528–1539.
[15] C.W. Peterson, S.S. Narula, I.M. Armitage, FEBS Lett. 379 (1996) 85–93.
[16] J.N. Butt, J. Niles, F.A. Armstrong, J. Breton, A.J. Thomson, Nat. Struct. Biol. 1 (1994) 427–433.
[17] A.K. Wernimont, D.L. Huffman, A.L. Lamb, T.V. O'Halloran, A.C. Rosenzweig, Nat. Struct. Biol. 7 (2000) 766–771.
[18] S. Hearnshaw, C. West, C. Singleton, L. Zhou, M.A. Kihlken, R.W. Strange, N.E. Le Brun, A.M. Hemmings, Biochemistry 48 (2009) 9324–9326.
[19] C. Singleton, S. Hearnshaw, L. Zhou, N.E. Le Brun, A.M. Hemmings, Biochem. J. 424 (2009) 347–356.
[20] A. Badarau, S.J. Firbank, A.A. McCarthy, M.J. Banfield, C. Dennison, Biochemistry 49 (2010) 7798–7810.
[21] C.J. Chen, M.Y. Liu, Y.T. Chen, J. LeGall, Biochem. Biophys. Res. Commun. 308 (2003) 684–688.
[22] J. Meyer, J. Gaillard, M. Lutz, Biochem. Biophys. Res. Commun. 212 (1995) 827–833.
[23] M. Cross, Z. Xiao, E.M. Maes, R.S. Czernuszewicz, S.C. Drew, J.R. Pilbrow, G.N. George, A.G. Wedd, J. Biol. Inorg. Chem. 7 (2002) 781–790.
[24] M. Kitamura, Y. Koshino, Y. Kamikawa, K. Kohno, S. Kojima, K. Miura, T. Sagara, H. Akutsu, I. Kumagai, T. Nakaya, Biochim. Biophys. Acta 1351 (1997) 239–247.
[25] M.K. Eidsness, A.E. Burden, K.A. Richie, D.M. Kurtz Jr., R.A. Scott, E.T. Smith, T. Ichiye, B. Beard, T. Min, C. Kang, Biochemistry 38 (1999) 14803–14809.
[26] M. Archer, A.L. Carvalho, S. Teixeira, I. Moura, J.J. Moura, F. Rusnak, M.J. Romao, Protein Sci. 8 (1999) 1536–1545.
[27] P. Saint-Martin, P.A. Lespinat, G. Fauque, Y. Berlier, J. Legall, I. Moura, M. Teixeira, A.V. Xavier, J.J. Moura, Proc. Natl. Acad. Sci. U. S. A. 85 (1988) 9378–9380.
[28] C. Ascenso, F. Rusnak, I. Cabrito, M.J. Lima, S. Naylor, I. Moura, J.J.G. Moura, J. Biol. Inorg. Chem. 5 (2000) 720–729.
[29] I. Moura, M. Teixeira, J. LeGall, J.J. Moura, J. Inorg. Biochem. 44 (1991) 127–139.
[30] R.E. Brown, K.L. Jarvis, K.J. Hyland, Anal. Biochem. 180 (1989) 136–139.
[31] M.J. Nilges, K. Matteson, R.L. Belford, SIMPOW6: a software package for the simulation of ESR powder-type spectra, in: M.A. Hemminga, L. Berliner (Eds.), ESR Spectroscopy in Membrane Biophysics, Biological Magnetic Resonance, Springer, New York, 2006, pp. 261–281.
[32] J. Meyer, J. Gagnon, J. Gaillard, M. Lutz, C. Achim, E. Munck, Y. Petillot, C.M. Colangelo, R.A. Scott, Biochemistry 36 (1997) 13374–13380.
[33] M. Bruschi, J. Le Gall, Biochim. Biophys. Acta Protein Struct. 263 (1972) 279–282.
[34] W.R. Hagen, EPR spectroscopy of iron–sulfur proteins, in: C. Richard (Ed.), Advances in Inorganic Chemistry, Academic Press, 1992, pp. 165–222.
[35] I. Moura, A.S. Pereira, P. Tavares, J.J.G. Moura, Simple and complex iron–sulfur proteins in sulfate reducing bacteria, in: A.G. Sykes (Ed.), Advances in Inorganic Chemistry, Academic Press, 1999, pp. 361–419.
[36] I. Moura, A. Macedo, J.J.G. Moura, EPR of iron–sulfur and mixed-metal clusters in proteins, in: A.J. Hoff (Ed.), Advanced EPR: Applications in Biology and Biochemistry, Elsevier, New York, 1989, pp. 813–838.
[37] A. Kr zel, W. Lesniak, M. Jezowska-Bojczuk, P. Mlynarz, J. Brasun, H. Kozlowski, W. Bal, J. Inorg. Biochem. 84 (2001) 77–88.

[38] T.E. Jones, D.B. Rorabacher, J. Am. Chem. Soc. 97 (1975) 7485–7486.
[39] C.A. Bell, P.V. Bernhardt, L.R. Gahan, M. Martinez, M.J. Monteiro, C. Rodriguez, C.A. Sharrad, Chemistry 16 (2010) 3166–3175.
[40] J. Peisach, W.E. Blumberg, Arch. Biochem. Biophys. 165 (1974) 691–708.
[41] J. Leckner, N. Bonander, P. Wittung-Stafshede, B.G. Malmstrom, B.G. Karlsson, Biochim. Biophys. Acta 1342 (1997) 19–27.
[42] A. Sandberg, D.J. Harrison, B.G. Karlsson, Biochemistry 42 (2003) 10301–10310.
[43] G. Chaka, J.L. Sonnenberg, H.B. Schlegel, M.J. Heeg, G. Jaeger, T.J. Nelson, L.A. Ochrymowycz, D.B. Rorabacher, J. Am. Chem. Soc. 129 (2007) 5217–5227.